

Induced microwave scattering in the ITER edge transport barrier at ECRH and possibility of its modeling at ASDEX-Upgrade

Evgeniy Gusakov, Alexei Popov, Michael Irzak

Ioffe Institute, 194021 Saint-Petersburg, Russia

Abstract. The induced scattering parametric decay instability of O-mode polarized microwaves leading to excitation of lower hybrid or electron plasma waves localized within a tokamak edge transport barrier is investigated. Numerical estimates of the instability threshold and its growth rate for this scenario are given for the conditions of O2-mode ECRH experiments at ASDEX-Upgrade, where experimental investigation of these phenomena is possible.

1 Introduction

Electron cyclotron resonance heating (ECRH) is widely used in current toroidal devices. The O1-mode ECRH technique is also considered for the local electron heating providing the neoclassical tearing mode control in ITER. Until very recently the propagation and absorption of O-mode microwaves were believed to be well-described by the linear theory and assumed to be predictable in detail. However, as it was shown in [1], in ITER they can suffer from a low threshold induced scattering parametric decay instability (PDI) in the edge transport barrier (ETB). The presence of a large density gradient have a significant impact on the properties of waves in the lower hybrid (LH) frequency range, leading to new transparency windows that are absent in a homogeneous plasma [2,3]. These new modes can be 2D localized along the direction of a plasma inhomogeneity due to gradient effects and along the magnetic field due to magnetic ripples. The instability power threshold leading to 2D localized LH or electron plasma (EP) wave excitation under the ITER conditions is much less than 1 MW. They are likely to be present in future O1-mode ECRH experiments at ITER and at DEMO, leading to broadening of the power deposition profile and therefore decreasing the neoclassical tearing mode suppression efficiency. Thus, the urgent experimental investigation of this parametric decay instability seems important for the ITER experiment planning. In the present paper we demonstrate a possibility to investigate the O-mode induced scattering PDI and its consequences in O2-mode ECRH experiments on ASDEX-Upgrade. The instability threshold is shown to be well below 0.5 MW. Its dependence on the density gradient in the ETB, magnetic field ripple and on the scattering angle is studied. The instability growth rate is also determined.

2 Lower hybrid and electron plasma waves in the edge transport barrier

To describe the behavior of LH and EP waves in the ETB with a proper account of magnetic field ripples we introduce the local Cartesian coordinate system (x, y, z) with its origin located at the inflection point of

the density profile and the local minimum of the magnetic field between two nearby coils. The coordinate x is related to the flux surface label, y is the coordinate perpendicular to the magnetic field line on the magnetic surface and z is the coordinate directed along the magnetic field line. We consider an electrostatic wave propagating mainly across the magnetic field on a magnetic surface, whose potential can be represented by means of the WKB approximation as $\phi = \Phi(x, z)\exp(iq_y y - i\omega_L t) + c.c.$ with its amplitude Φ obeying the Poisson equation

$$\hat{D}(\omega_L)\Phi = \varepsilon(\omega_L)\left(\frac{\partial^2}{\partial x^2} - q_y^2\right)\Phi + \frac{\partial g(\omega_L)}{\partial x}q_y\Phi + \eta(\omega_L)\frac{\partial^2}{\partial z^2}\Phi = 0 \quad (1)$$

where ε , g , η are the cold-plasma dielectric tensor components; ω_{pi} and ω_{pe} - the ion and electron plasma frequencies; ω_{ci} and ω_{ce} - the ion and electron cyclotron frequencies. Then, we introduce a function $Q = \varepsilon(\omega_L)^{-1} \partial g(\omega_L) / \partial x$ which has a local maximum at the inflection point of the density profile in the ETB region leading to a localized solution around $x=0$. Figure 1 shows the typical density profile (thick solid curve) at an ETB in the ASDEX-Upgrade. The solid curve shows the wave number $q_x = q_x(q_y, q_z = 0)$ of the LH wave ($f_L = 2.8$ GHz, $q_y = Q_0/2 = 2.4$ cm⁻¹, $Q_0 = Q(0,0)$). To describe this localized solution analytically, we expand the magnetic field in powers of z around the magnetic field minimum position $B \approx \bar{B}\left(1 - \delta(x, y)(Nz/R)^2/2 + \dots\right)$, where \bar{B} is the magnetic field on a given magnetic surface, N is the number of toroidal field coils, R is the tokamak major radius; and δ is the amplitude of magnetic ripples. This allows approximating the function Q with a parabola over both coordinates $Q \approx Q_0\left(1 - \frac{x^2}{2l_x^2} + \frac{z^2}{2l_z^2}\right)$ and reducing equation (1) to

$$\left(\varepsilon(\omega_L, 0)\left(\frac{\partial^2}{\partial x^2} + Q_0 q_y - q_y^2 - K_x^4 x^2\right) - \left|\eta(\omega_L, x_m)\left(\frac{\partial^2}{\partial z^2} - K_z^4 z^2\right)\right|\right)\Phi = 0 \quad (2)$$

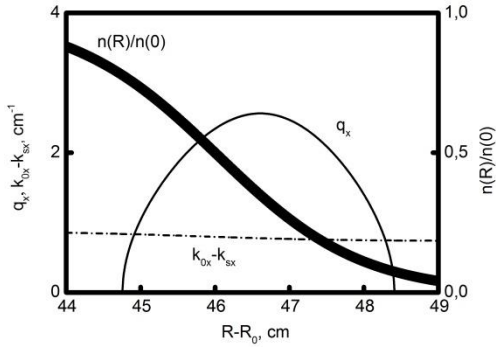


Fig. 1. Dispersion curves of the interacting waves. The thick solid curve shows the dimensionless density. The dashed dotted curve is the difference between the numbers of the pump and scattered O-mode waves $k_{0x} - k_{sx}$. The solid curve is the EP wave number $q_x = q_x(q_{ym}, q_z = 0)$, $q_{ym} = 2.4 \text{ cm}^{-1}$. The pump and scattered wave frequencies are $f_0 = 140 \text{ GHz}$, $f_s = 137.02 \text{ GHz}$; the scattering angle is $\vartheta = 5.3^\circ$; $\Delta_{\text{ETB}} = 2 \text{ cm}$.

where $K_x = (Q_0 q_y / (2l_x^2))^{1/4}$, $K_z = (Q_0 q_y / (2l_z^2 |\eta(\omega_L)|))^{1/4}$. Equation (2) describes a wave localized both in the radial direction and along the magnetic field and has a solution $\Phi(\mathbf{r}) = \Phi_{p,r} f_p(K_x x) f_r(K_z z)$, expressed in terms of the Hermite polynomials $f_p(Kx) = \sqrt{K / (\sqrt{\pi} 2^p p!)} \exp(-K^2 x^2 / 2) H_p(Kx)$ with the amplitude $\Phi_{p,r}$ taken constant. The eigenfrequency of the 2D trapped wave is determined by the following equation

$$\kappa^2 (\omega_{L,r}^{p,r}) = (2r+1) |\eta(\omega_{L,r}^{p,r})| K_z^2 (\omega_{L,r}^{p,r}) + \varepsilon(\omega_{L,r}^{p,r}) (Q_0 (\omega_{L,r}^{p,r}) q_y - q_y^2 - (2p+1) K_x^2 (\omega_{L,r}^{p,r})) = 0 \quad (3)$$

If the density gradient is small, or even absent, the plasma is evanescent for such a LH wave propagating almost perpendicular to the external magnetic field. However, in the case of strongly inhomogeneous plasmas the new transparency regions for LH waves appear first discovered in [2]. Later, it was demonstrated numerically [3] that at large density gradients these oscillations, propagating strictly across the magnetic field, can be localized in the plasma inhomogeneity direction. It should be noted that this wave has a remarkable property. In a certain range of wave numbers q_y , it changes the sign of its group velocity v_{gy} in the y direction within the localization region along the direction of the plasma inhomogeneity. When $q_{ym} = Q_0 / 2 (1 - (2p+1) / (4K_x^2 l_x^2))$, the average convection velocity along the y coordinate is zero $u_{Ly} = \int_{-\infty}^{\infty} dx |f_p(K_x x)|^2 v_{gy}(x) = 0$. For such a wave, the convective loss along the y direction is suppressed and the only sink of its energy from the decay region is due to diffraction. The latter is a slower process than convection. The LH or EP wave possessing a y wave number close to the optimal value q_{ym} is the most unstable when excited due to a PDI.

3 O-mode induced scattering off LH or EP waves 2D localized in an ETB

In inhomogeneous plasmas the parametric decay occurs in a narrow layer in the close vicinity of a point at which the decay resonance for the frequencies and numbers of coupled oscillations are fulfilled. We assume that the decay point is within the ETB and consider a pump O-mode wave propagating perpendicular to the magnetic field along x towards the plasma core. The pump wave can decay into a localized LH wave and an O-mode wave. The potential of the LH wave without the nonlinear coupling is described by equation (2). Its frequency and wave number obey the quantization condition (3). We assume that the y component of the LH wave number is equal to the optimal value. As decay begins, the amplitude $\Phi_{p,r}$ of the non-linearly excited LH or EP wave starts to grow in the pump localization zone and experiences diffraction along y . According to [1], this phenomenon is described by the following equation

$$\left(\frac{\partial}{\partial t} + i < \Lambda_y > \frac{\partial^2}{\partial y^2} \right) \Phi_{p,r} = \gamma_0 \exp\left(-\frac{y^2}{\tilde{w}^2}\right) \Phi_{p,r} \quad (4)$$

where $< \Lambda_y > = \int_{-\infty}^{\infty} |f_p(K_x x)|^2 |f_r(K_z z)|^2 \Lambda_y dx dz$ is the diffraction coefficient averaged over the wave localization area, $\tilde{w}^2 = |w^2|^2 / w_0^2$, $w = \sqrt{w_0^2 - i R_f c / \omega_0}$ is the local complex width of a beam, w_0 is the beam width at the focus position x_f , the parameter R_f when it obeys the inequality $w_0^2 \gg R_f c / \omega_0$ has the meaning of a wavefront curvature radius at the antenna,

$$\gamma_0 = \frac{A_0^2}{8B(0)^2} \frac{\omega_{pe}^4(0)}{\omega_0^2 \omega_{ce}^2(0)} \frac{c}{\omega_s} \frac{1}{< \partial D(\omega_L) / \partial \omega >} \times \frac{(q_{ym}^2 + K_x^2 (2p+1))^2}{n_{sx}(0) n_{0x}(0)} \int_{-\infty}^{\infty} dz \exp\left(-\frac{z^2}{\tilde{w}^2}\right) |f_r(K_z z)|^2 \times \quad (5)$$

$$\int_{-\infty}^{\infty} dx f_p(K_x x)^* \int_{-\infty}^x dx' \exp\left(i \int_{x'}^x \Delta K dx''\right) f_p(K_x x')$$

is the pumping rate; $\omega_0, \omega_s = \omega_0 - \omega_{L,r}^{p,r}$ are the pump and scattered O-mode frequencies, $\Delta K = (\omega_{sx} n_{sx} - \omega_{0x} n_{0x}) / c$; $n_{0,xx} = n_x(\omega_{0,s}, n_{0,xy})$, $n_x(\omega_0, n_y) = \sqrt{\eta(\omega_0) - n_y^2}$, P_0 and $A_0 = \sqrt{8P_0 / (c\tilde{w}^2)}$ are the pump wave's power and amplitude. If the pump power significantly exceeds the power threshold value, *i.e.* $P_0 \gg P_0^{\text{th}}$, then we can approximate solution to (4) analytically (see [4]) $\Phi_{p,r}(t, y) = \exp(\gamma_{ins}^s t + i \delta \omega_{ins}^s t) f_s(K_y y)$, $s \in Z$, where

$$K_y^{-1} = \frac{< \Lambda_y >^{1/4} \tilde{w}^{1/2}}{\sqrt[4]{\gamma_0}} \exp\left(-i \frac{\pi}{8} - i \arg\left(\frac{\gamma_0}{4}\right)\right), \quad (6)$$

$$\delta \omega_{ins}^s = \gamma_0'' + (2s+1) \sqrt{\frac{|\gamma_0| < \Lambda_y >}{\tilde{w}^2}} \cos\left(\frac{\arctan(\gamma_0'' / \gamma_0')}{2} + \frac{\pi}{4}\right)$$

and

$$\gamma_{ins}^s = \gamma_0' - (2s+1) \sqrt{\frac{|\gamma_0| < \Lambda_y >}{\tilde{w}^2}} \sin\left(\frac{\arctan(\gamma_0'' / \gamma_0')}{2} + \frac{\pi}{4}\right)$$

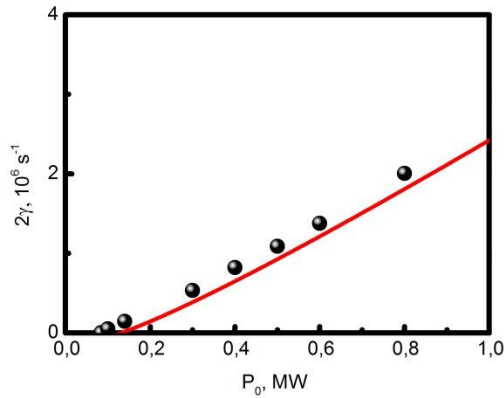


Fig. 2. Dependence of the growth rate on the pump power. The solid curve is defined by the analytical dependence (6). The scattered circles are the results of numerical solution of equation (4). The numerical solution gives an estimate for the power threshold of $P_0^{th} = 0.094$ MW at $\delta = 0.5\%$, $w = 2$ cm and the same parameters of the coupled waves as in figure 1.

is the LH wave growth rate. Though equation (6) is no more valid if the pump power only slightly exceeds the threshold value $P_0 \geq P_0^{th}$, we can use it to derive a rough estimate of the PDI threshold

$$\gamma_0'(P_0^{th}) = (2s + 1) \sqrt{\frac{|\gamma_0(P_0^{th})| < \Lambda_y >}{\tilde{w}^2}} \times \sin\left(\frac{\arctan(\gamma_0''(P_0^{th}) / \gamma_0'(P_0^{th}))}{2} + \frac{\pi}{4}\right) \quad (7)$$

4 Induced scattering PDI for O2-mode ECRH in ASDEX-Upgrade

The induced scattering PDI can be investigated in O2-mode ECRH experiments at the ASDEX-Upgrade tokamak ($R_0 = 165$ cm, a central magnetic field is up to 3T, $N = 16$) proposed for central heating of dense plasma [5]. For the parameters of O2-mode ECRH at ASDEX-Upgrade with 140 GHz gyrotrons the single pass absorption is incomplete [6] which provides a chance of measuring of the induced forward-scattering signal at the high magnetic field side of the device after crossing the resonance layer. The magnetic ripple amplitude at the separatrix is 0.2 - 1%, depending on its position [7]. Thus, if such experiments were carried out with ETB parameters similar to those discussed in [8], the phenomenon analyzed in this article could occur. To prove this, we plot in figure 1 the dispersion curves of the LH wave (thin solid curve) along with a difference of the pump and forward scattered O-mode wave numbers (dashed dotted curve). The pump and scattered O-mode wave frequencies are $f_0 = 140$ GHz and $f_s = 137.02$ GHz. The y component of the wave number is $q_{ym} = 2.4$ cm $^{-1}$, that corresponds to a local scattering angle of $\vartheta = \tan(q_{ym} / k_{ox})^{-1} = 5.3^\circ$. Since the O2-mode does not experience strong absorption in the optically thin ECR layer [6], the scattering signal can be detected on the high magnetic field side.

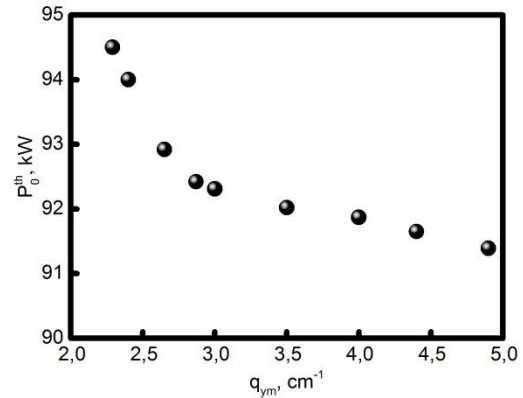


Fig. 3. Dependence of the instability threshold, which is determined numerically by solving equation (4), on the parameter q_{ym} at an eigenfrequency corresponding to this value. The other parameters are the same as in figure 2.

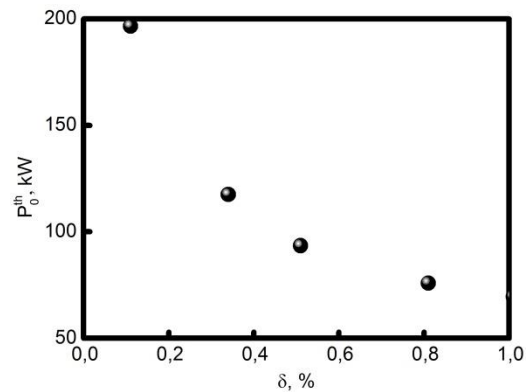


Fig. 4. Dependence of the power threshold on the ripple amplitude. The other parameters are the same as in figure 2.

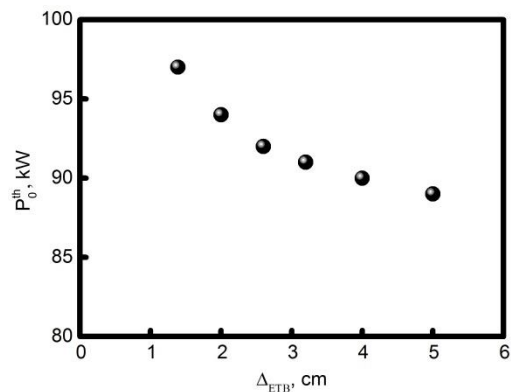


Fig. 5. Dependence of the instability threshold, which is determined numerically, on the inhomogeneity scale Δ_{ETB} at the density profile inflection point x_{inf} and at $q_{ym} = 2.4$ cm $^{-1}$. The other parameters are the same as in figure 2.

Figure 2 shows the dependence of the growth rate on the pump power. The solid curve is given by (6). The scattered circles are the results of numerical solution of (4). According to (8), the predicted instability threshold is $P_0^{th} = 0.131$ MW, while the numerical solution gives a value of $P_0^{th} = 0.094$ MW for it. The ripple amplitude here

was assumed to be $\delta = 0.5\%$, while the pump beam width was assumed to be $\tilde{w} = 2$ cm. Figure 3 shows a weak dependence of the instability threshold, which is determined numerically, on the parameter q_{ym} at the eigenfrequency (3) corresponding to this optimum value. The other parameters are the same as in figure 1. Figure 4 shows the dependence of the instability threshold calculated numerically on the ripple amplitude. Increasing the ripple amplitude reduces the LH wave localization area along the magnetic field. The latter increases the coupling efficiency and decreases the instability threshold. Figure 5 shows the dependence of the instability threshold, which is determined numerically, on the inhomogeneity scale Δ_{ETB} at the density profile inflection point x_{inf} in the ETB and at $q_{ym} = 2.4 \text{ cm}^{-1}$. The dependence in figure 5 on the scale of inhomogeneity Δ_{ETB} is also weak. It remains to be noted that all figures 1-5 are plotted for the parameters at the inflection point of the density profile as follows $B_0 = 2.5$ T, $n(x_{\text{inf}}) = 0.7 \times 10^{14} \text{ cm}^{-3}$, $T_{e,i}(x_{\text{inf}}) = 200$ eV.

5 Conclusions

In the present work we have shown that an absolute induced scattering parametric decay instability, leading to the excitation of a lower hybrid wave localized in the edge transport barrier, may be investigated in the proposed O2-mode ECRH experiments on the ASDEX-Upgrade tokamak. We have estimated the instability threshold and shown that it is significantly lower than the power available in a single microwave beam. The growth rate of instability and spectral characteristics of the scattering signal in the proposed experiments were also discussed. However, in order to predict the power level of induced scattering, a study of the instability saturation is needed, which is planned by the authors and will be implemented in the future.

The analytical treatment is supported under the RSF 22-12-00010 grant, the numerical modelling is performed under the Ioffe Institute state contract 0040-2019-0023 whereas the code for the PDI modeling was developed under the Ioffe Institute state contract 0034-2021-0003.

References

1. E.Z. Gusakov, A.Yu. Popov, Phys. Rev. Lett. **128**, 065001 (2022)
2. E.Z. Gusakov, M.A. Irzak, A.D. Piliya, JETP Letters **65**, 25 (1997)
3. E.Z. Gusakov, V.V. Dyachenko, M.A. Irzak, O.N. Shcherbinin, S.A. Khitrov, Plasma Phys. Control. Fusion **52**, 075018 (2010)
4. E.Z. Gusakov, A.Yu. Popov, Phys. Usp. **63**, 365 (2020) <https://doi.org/10.3367/UFNe.2019.05.038572>
5. M. Schubert et al. and the ASDEX Upgrade Team, Proceedings of 43rd EPS Conference on Plasma

Physics 4 - 8 July 2016, Leuven, Belgium Vol **40A** (ISBN: 2-914771-99-1), P1.026

6. V. Ereckmann, U. Gasparino, Plasma Phys. Control. Fusion **36**, 1869 (1994)
7. M. Garcia-Munoz et al. and the ASDEX Upgrade Team, Plasma Phys. Control. Fusion **55**, 124014 (2013)
8. W. Tierens et al. and the ASDEX Upgrade Team, Nucl. Fusion **57**, 116034 (2017)